35. Sawa M. Measurement of corneal thickness. Jap Rev Clin Ophthalmol (Ganka Rinsho Iho) 1986;80:177–184.
36. Muir KW, Jin J, Freedman SF. Central corneal thickness and its relationship to intraocular pressure in children. Ophthalmology 2004;111:2220–2223.
37. Kao SF, Lichter PR, Bergstrom TJ, et al. Clinical comparison of the Oculab Tono-Pen to the Goldmann applanation tonometer. Ophthalmology 1987;94:1541–1544.
38. Bordon AF, Katsumi O, Hirose T. Tonometry in pediatric patients: a comparative study among Tono-pen, Perkins, and Schiotz tonometers. J Pediatr Ophthalmol Strabismus 1995;32:373–377.
39. Dohadwala AA, Munger R, Damji KF. Positive correlation between Tono-Pen intraocular pressure and central corneal thickness. Ophthalmology 1998;105:1849–1854.
40. Bhan A, Browning AC, Shah S, et al. Effect of corneal thickness on intraocular pressure measurements with the pneumotonometer, Goldmann applanation tonometer, and Tono-Pen. Invest Ophthalmol Vis Sci 2002;43:1389–1392.
41. Yildirim N, Sahin A, Basmak H, Bal C. Effect of central corneal thickness and radius of the corneal curvature on intraocular pressure measured with the Tono-Pen and noncontact tonometer in healthy schoolchildren. J Pediatr Ophthalmol Strabismus 2007;44: 216–222.
42. Dominguez A, Banos S, Alvarez G, et al. Intraocular pressure measurement in infants under general anesthesia. Am J Ophthalmol 1974;78:110–116.

Jpn J Ophthalmol 2009;53:12–17

DOI 10.1007/s10384-008-0602-2

CLINICAL INVESTIGATION

Age-Related Changes of Phoria Myopia in Patients with Intermittent Exotropia

Hiroshi Shimojyo[1], Yoshiyuki Kitaguchi[2], Sanae Asonuma[1], Kenji Matsushita[1], and Takashi Fujikado[2]

[1]Department of Ophthalmology, Osaka University Medical School, Osaka, Japan;
[2]Department of Applied Visual Science, Osaka University Medical School, Osaka, Japan

Abstract

Purpose: To investigate the age-related changes in a myopic shift under binocular conditions (phoria myopia) in patients with intermittent exotropia (IXT).

Methods: Forty-five patients with IXT were studied: 21 were ≤9 years old (children), 11 were between 10 and 19 years (adolescents), and 13 were between 20 and 43 years (adults). The angle of strabismus was determined by the alternating prism cover test. The spherical refractive error was measured at 1 m using infrared video retinoscopy under monocular and binocular viewing conditions.

Results: The change in the spherical refractive error (ΔR) between binocular and monocular conditions was significantly larger in adults (ΔR = −1.11 ± 1.01 diopters (D), average ± standard deviation) than in children (ΔR = −0.34 ± 0.34 D; $P < 0.05$, analysis of variance). ΔR was significantly correlated with the angle of exotropia only in adults ($r = 0.55$, $P = 0.04$). After strabismus surgery, ΔR decreased in adults ($n = 3$).

Conclusions: Because a significant myopic shift under binocular conditions was detected in IXT patients older than 20 years, phoria myopia can occur after age 20 even if functional disturbances are not observed in children or adolescent IXT patients, a fact that specialists need to bear in mind when treating younger patients. **Jpn J Ophthalmol** 2009;53:12–17 © Japanese Ophthalmological Society 2009

Key Words: aging, intermittent exotropia, myopic shift, phoria myopia, pupil constriction

Introduction

In adults with intermittent exotropia (IXT), a myopic shift and miosis are observed when the visual system switches from monocular to binocular viewing conditions.[1–5] A significant myopic shift under binocular conditions in IXT with a relatively large angle is called "phoria myopia" in Japan. Phoria myopia was first named by K. Yuge in Japanese and by K. Adachi in English.[4,5]

Received: March 5, 2008 / Accepted: July 31, 2008
Correspondence and reprint requests to: Takashi Fujikado, Department of Applied Visual Science, Osaka University Graduate School of Medicine, 2-2 Yamadaoka, Suita, Osaka 565-0871, Japan
e-mail: fujikado@ophthal.med.osaka-u.ac.jp

The miosis in the near reflex is reported to be larger in normal subjects >20 years old than in those ≤20 years.[6] However, the relationship between age and the myopic shift or pupillary constriction in patients with IXT has not been well investigated.

The relationship between convergence (C) and accommodation (A) is principally linear (AC/A or CA/C ratio) under open-loop conditions, in which either a convergence or an accommodation cue is present. However, it is not linear under closed-loop conditions, in which both cues are present. In patients with IXT, a greater effort to converge is required to fixate a near target binocularly compared with patients with orthophoria. Therefore, a greater myopic shift and miosis can be expected under exophoric (binocular) than under exotropic (monocular) conditions, especially if the angle of strabismus is large and the connection between convergence and accommodation in the central nervous system is rigid.

Ophthalmic Genetics, 29:29–32, 2008

ISSN: 1381-6810 (print) / 1744-5094 (online)
DOI: 10.1080/13816810701663535

informa
healthcare

CASE REPORT

Novel *RDH5* Mutation in Family with Mother Having Fundus Albipunctatus and Three Children with Retinitis Pigmentosa

Chunxia Wang
Department of Ophthalmology, Hamamatsu University School of Medicine, Hamamatsu, Japan, and Medical Photobiology Department, Photon Medical Research Center, Hamamatsu University School of Medicine, Hamamatsu, Japan

Nobuo Nakanishi and Kentaro Ohishi
Medical Photobiology Department, Photon Medical Research Center, Hamamatsu University School of Medicine, Hamamatsu, Japan

Akiko Hikoya, Kenro Koide, and Miho Sato
Department of Ophthalmology, Hamamatsu University School of Medicine, Hamamatsu, Japan

Makoto Nakamura
Department of Ophthalmology, Nagoya University School of Medicine, Nagoya, Japan

Yoshihiro Hotta
Department of Ophthalmology, Hamamatsu University School of Medicine, Hamamatsu, Japan

Shinsei Minoshima
Medical Photobiology Department, Photon Medical Research Center, Hamamatsu University School of Medicine, Hamamatsu, Japan

***Purpose*: To identify mutations in the *RDH5* gene in a family with a mother having fundus albipunctatus (FA) and 3 children with retinitis pigmentosa (RP). *Methods*: Ophthalmological examinations were performed to diagnose FA and RP. Mutational analysis of *RDH5* was performed. *Results/Conclusions*: The mother was diagnosed with FA, and 3 children were diagnosed with RP. The proband's mother, brother, and sister had a novel mutation c.689_690CT>GG in *RDH5*. The proband and mother had a previously reported mutation c.928delCinsGAAG. Consequently, the mother's FA was caused by compound heterozygous mutations. Further studies will be needed to determine the gene responsible for children's RP.**

Keywords fundus albipunctatus; retinitis pigmentosa; night blindness; RDH5 gene; mutation

INTRODUCTION

Fundus albipunctatus (FA) is an autosomal recessive disease and is characterized by the presence of numerous small white dots throughout the retina and congenital stationary night blindness. FA is caused by mutations of the *RDH5* gene in most cases.[1] In Japanese cases of FA, a c.928delCinsGAAG mutation has been detected in many families suggesting a founder effect.[2–6] We describe an unusual family which included a mother with FA and three children with typical retinitis pigmentosa (RP). We examined the *RDH5* genotype of this family and found a novel mutation.

Received 13 July 2007; accepted 3 September 2007.
Address correspondence to Shinsei Minoshima, Professor, Medical Photobiology Department, Photon Medical Research Center, Hamamatsu University School of Medicine, 1-20-1 Handayama, Hamamatsu, 431-3192, Japan. E-mail: mino@hama-med.ac.jp

MATERIALS AND METHODS

Patients

A 12-year-old young girl (proband, patient P1, Fig. 1) was referred to our hospital with a tentative diagnosis of RP. She had

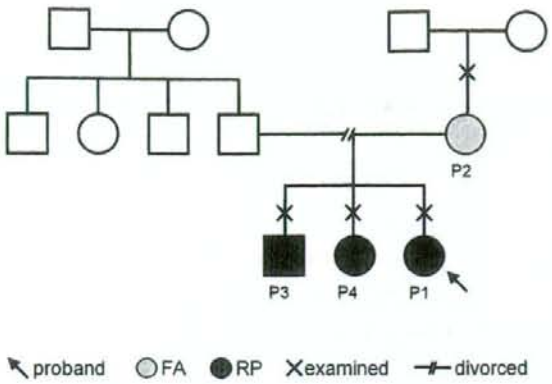

FIG. 1. Pedigree of a family with fundus albipunctatus (FA) and retinitis pigmentosa (RP). All affected patients complained of night blindness.

complained of night blindness since 7 years of age. Her best-corrected visual acuity was 1.0 in both eyes, and her peripheral visual fields were mildly constricted. Funduscopic examination revealed numerous bone-spicule pigments, a typical appearance of eyes with RP (Fig. 2A). The a- and b-waves of single flash ERGs were severely reduced (data not shown).

The proband's mother (P2, 43-year-old) also complained of night blindness. She was being treated by several medications for iron deficiency anemia and hypertension. Her best-corrected visual acuity was 0.9 OD and 1.0 OS, and her visual fields were normal. Funduscopic examination showed numerous yellow-white punctuate deposits around the vascular arcades without a central macular involvement (Fig. 2A). The scotopic, full-field ERGs were markedly reduced but recovered to normal levels after 120 minutes of dark-adaptation (Fig. 2B). The recovery of the ERG amplitudes following prolonged dark-adaptation is pathognomonic of eyes with FA.

The proband's brother (P3, 19-year-old) and sister (P4, 18-year-old) also complained about night blindness. The best-corrected visual acuity was 1.0 in both eyes of both siblings. A mild peripheral visual field constriction was detected in P3 and a ring scotoma in P4. Although funduscopic examination revealed pigment deposits in the mid-peripheral retina in P3, fluorescein angiography showed a broad window defect due to retinal pigment epithelium atrophy around the vascular arcades without central macular involvement. Numerous bone-spicule

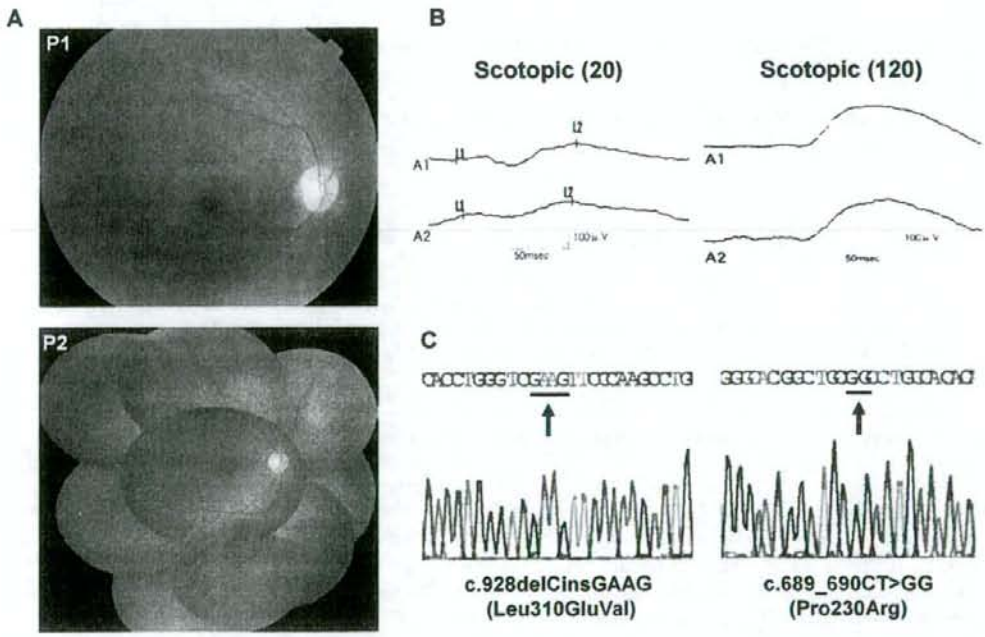

FIG. 2. Results of clinical examination and detected mutations in the family. A. Fundus photographs of P1 showing numerous bone-spicule pigments in the peripheral retina, and P2 showing numerous yellow-white punctuate deposits around the vascular arcades without central macular involvement. B. Scotopic ERGs of P2, showing markedly reduced scotopic response which recovered after 120 minutes of dark-adaptation. C. Mutations found in this family. Left, c.928delCinsGAAG in P1 and P2; right, c.689_690CT>GG in P2, P3 and P4. The other alleles of P1, P3, and P4 are normal (data not shown). Notation of mutation is done according to Nomenclature system by MDI.[12] Bars and arrows indicate the position of the mutations.

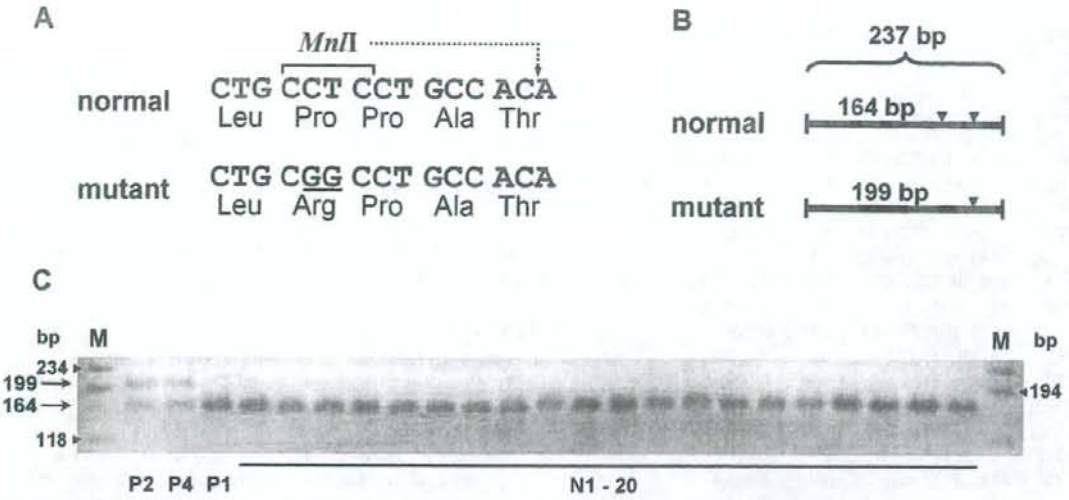

FIG. 3. Restriction endonuclease analysis for a novel mutation, c. 689_690CT>GG. A. Partial sequences of exon 4 of the normal allele and the mutant allele. The recognition site of *MnlI* (CCTC) existing in the relevant position of normal allele is not present in the mutated gene. Dotted arrow indicates the cutting site. B. *MnlI* sites (arrowheads) on the amplified DNA (237 bp) of exon 4 and its surrounding introns. The DNA derived from the mutant allele should not be cut at the mutation site, but the normal allele should be at the corresponding site to produce a 164-bp fragment. Another *MnlI* site (right) exists in both mutant and normal alleles. C. Results of restriction endonuclease analysis using PCR-amplified DNA from three patients (P1, P2, P4) and unaffected controls (N1 through 20). Only DNA from P2 and P4 produced 199-bp fragment of mutation. The 164-bp fragment was detected in P1, P2, P4 and controls. M = DNA size marker; arrowheads indicate the position of marker and arrows indicate the position of the produced DNA fragments.

pigments were observed in the retina of P4. The a- and b-waves of the single flash ERGs were severely reduced in both siblings (data not shown).

Mutation Analyses

This study was approved by the Institutional Review Board for Human Genetic and Genomic Research of Hamamatsu University School of Medicine, and the procedures used conformed to the tenets of the Declaration of Helsinki. Informed consent was obtained from the patients and unrelated normal controls. Genomic DNA was isolated from peripheral blood leukocytes. The regions corresponding to the protein-coding exons, exon 2–5, of the *RDH5* gene were amplified by PCR using primers previously described.[1] The PCR products were sequenced on an Applied Biosystems model 3100 automated sequencer (Perkin-Elmer, Foster City, CA, USA) with primers that were used for the PCR amplification. For the cases which had some sequence abnormality, both alleles were cloned using pBLUESCRIPT II SK(+) vector (Stratagene, La Jolla, CA) to examine their sequences separately.

RESULTS AND DISCUSSION

A novel 2-base missense mutation c.689_690CT>GG (Pro230Arg) in exon 4 (Fig. 2C) was found in P2, P3, and P4, and was not detected in the normal controls using restriction endonuclease *MnlI* digestion of PCR-amplified DNAs (Fig. 3). This confirmed that c.689_690CT>GG is a pathogenic mutation and not a polymorphism. This type of mutation (missense by 2 consecutive base change) is very rare. Until this article, we were able to find 25 kinds of this type of mutation in 15 genes in all of the 1,700 disease-causing genes (see mutation databases *MutationView*[7] and HGMD[8]).

All of this type of mutation are listed in the Table 1 including our case. Of these, the change from CT to GG of the *RDH5* gene in our patient is the first case. The complementary change (AG to CC) was not found. This mutation of *RDH5* is the first one in all known missense mutations in human disease-causing genes. Mutations of 2 base or more are considered to be caused by the failure in the repair of DNA lesion or replication errors, in which various mechanisms should work, such as nucleotide excision repair, mismatch repair or homologous recombination mediated repair.[9]

However, it is not known if a particular mechanism exists for 2 consecutive base pair changes. In this table, transversions are found more frequently than transitions, 32 *vs.* 20 (Table 1). This is interesting because transition mutations are found more than transversions in cases of single base change mutations, suggesting that something related to the generation mechanism of this type of mutation. Further studies are necessary to analyze this type of mutation.

TABLE 1
Summary of reported 2 consecutive base mutations

# Gene	Gene symbol	Mutation	Type*	Amino acid change
1	ARSA	286_287TC>CT	SS	S96L
2	ATM	7875_7876TG>GC	VV	D2625_A2626indelEP
	ATM	8565_8566TG>AA	VS	S2855_V2856indelRI
3	CFTR	1294_1295AC>TA	VV	T388X
	CFTR	2916_2917TC>AT	VS	L973F
4	CNGB3	1573_1574TT>AA	VV	F525N
5	DYSF	200_201TG>AT	VV	V67D
	DYSF	3444_3445TG>AA	VS	Y1148X
6	F9	1092_1093TA>CG	SS	S365G
7	GJB1	64_65CG>TA	SS	R22X
8	IL2RG	536_537TG>AA	VS	L179X
9	KCNE1	152_153TG>AT	VV	L51H
	KCNE1	176_177TG>CT	SV	L59P
10	MLH1	531_532GG>AT	SV	E178X
	MLH1	1852_1853AA>GC	SV	K618A
	MLH1	1852_1853AA>CG	VS	K618R
11	NF1	945_946GC>AA	SV	L316M
	NF1	4861_4862GT>AG	SV	V1621R
	NF1	7424_7425CT>AG	VV	S2475X
12	NPHP4	1334_1335TC>AA	VV	F445X
13	NR5A1	104_105GC>AA	SV	G35E
14	PAH	470_471GA>AC	SV	R157N
	PAH	796_797AC>GA	SV	T266E
15	PAX6	363_364AT>CA	VV	M1Q
	PAX6	862_863CG>GA	VS	S167X
16	RDH5	689_690CT>GG	VV	P230R

*Types of 2 consecutive mutations are shown in S (transition) or V (transversion). Total S and V are 20 and 32, respectively.

Another mutation found in P1 and P2 was c.928delCins GAAG (Leu310GluVal) in exon 5 (Fig. 2C), which has been reported in many cases of FA.[2–6] Consequently, the FA of P2 was most likely caused by compound heterozygous mutations of *RDH5*, viz., c.689_690CT>GG and c.928delCinsGAAG.

Only two reports have been published on families with both FA and RP. Kuroiwa *et al* reported a family which included a FA patient with compound heterozygous *RDH5* mutations (Val177Gly and Arg280His) and a family member with RP without a mutation in the gene.[10] Sato and colleagues described a case of FA associated with sectorial RP in the inferonasal retinal quadrants of both eyes, in which a homozygous RDH5 mutation (Gly107Arg) was found.[11] To the best of our knowledge, our family is the first with a mother with FA and 3 children with typical RP. Further studies will be needed to determine the responsible genetic defects for the RP of the 3 children of this family.

ACKNOWLEDGMENTS

This work was supported in part by a Grant-in-Aid for Scientific Research on Priority Areas from the Ministry of Education, Culture, Sports, Science and Technology (MEXT) and a Grant-in-Aid for Scientific Research from the Japan Society for the Promotion of Science (JSPS).

Chunxia Wang is a scholarship student of the Japanese Government (Monbukagakusho:MEXT) (2003–2007).

REFERENCES

1. Yamamoto H, Simon A, Eriksson U, Harris E, Berson EL, Dryja TP. Mutations in the gene encoding 11-*cis* retinol dehydrogenase cause delayed dark adaptation and fundus albipunctatus. *Nat Genet.* 1999;22:188–191.
2. Nakamura M, Hotta Y, Tanikawa A, Terasaki H, Miyake Y. A high association with cone dystrophy in fundus albipunctatus caused by mutations of the *RDH5* gene. *Invest Ophthalmol Vis Sci.* 2000;41:3925–3932.
3. Hirose E, Inoue Y, Morimura H, Okamoto N, Fukuda M, Yamamoto S, Fujikado T, Tano Y. Mutations in the 11-cis retinol dehydrogenase gene in Japanese patients with fundus albipunctatus. *Invest Ophthalmol Vis Sci.* 2000;41:3933–3935.
4. Sekiya K, Nakazawa M, Ohguro H, Usui T, Tanimoto N, Abe H. Long-term fundus changes due to fundus albipunctatus associated with mutations in the *RDH5* gene. *Arch Ophthalmol.* 2003;121:1057–1059.
5. Wada Y, Abe T, Fuse N, Tamai M. A frequent 1085delC/insGAAG mutation in the *RDH5* gene in Japanese patients with fundus albipunctatus. *Invest Ophthalmol Vis Sci.* 2000;41:1894–1897.
6. Nakamura M, Miyake Y. Macular dystrophy in a 9-year-old boy with fundus albipunctatus. *Am J Ophthalmol.* 2002;133:278–280.
7. Minoshima S, Mitsuyama S, Ohtsubo M, Kawamura T, Ito S, Shibamoto S, Ito F, Shimizu N. The KMDB/MutationView: A mutation database for human disease genes. *Nucl Acids Res.* 2001;29:327–328.
8. Cooper DN, Ball EV, Krawczak M. The human gene mutation database. *Nucleic Acids Res.* 1998;26:285–287.
9. Moustacchi E. DNA damage and repair: consequences on dose-responses. *Mutat Res.* 2000;464:35–40.
10. Kuroiwa S, Kikuchi T, Yoshimura N. A novel compound heterozygous mutation in the *RDH5* gene in a patient with fundus albipunctatus. *Am J Ophthalmol.* 2000;130:672–675.
11. Sato M, Oshika T, Kaji Y, Nose H. A novel homozygous Gly107Arg mutation in the RDH5 gene in a Japanese patient with fundus albipunctatus with sectorial retinitis pigmentosa. *Ophthalmic Res.* 2004;36:43–50.
12. den Dunnen JT, Antonarakis SE. Mutation nomenclature extensions and suggestions to describe complex mutations: A discussion. *Hum Mutat.* 2000;15(1):7–12.

顕微鏡下における立体視機能の検討

Evaluation of stereopsis under the microscope

平井教子[1*]・阿曽沼早苗[1]・大澤　結[1]・天野大輔[1]・高田雄介[1]・
鶴留康弘[2]・藤木かおり[3]・天野知子[4]・下條裕史[1]・不二門 尚[5]

Kyoko Hirai[1*]・Sanae Asonuma[1]・Yui Osawa[1]・Daisuke Amano[1]・Yusuke Takada[1]・
Yasuhiro Tsurudome[2]・Kaori Fujiki[3]・Tomoko Amano[4]・Hiroshi Shimojo[1]・Takashi Fujikado[5]

【要約】 目的：顕微鏡下で奥行き感を測定できる三杆法(M三杆法)装置を試作し，顕微鏡下で立体感が得られにくいケースの要因を検討した．

対象および方法：Titmus Stereo Test(TST)で40秒の立体視を有する33例に対して，M三杆法でのズレ量(片眼視下および両眼視下)を測定した．また，顕微鏡下でのTST，非顕微鏡下のTNO Stereo Test(TNO)，調節幅，融像幅，AC/A比を測定し，M三杆法の結果と比較検討した．

結果：M三杆法でのズレ量は，片眼視下と比較して両眼視下で有意に少なかった．また，TNOの成績が不良のケースでは，M三杆法でのズレ量も大きく，両者は有意な相関を示したが，他の検査結果との比較では有意な関係はみられなかった．M三杆法でのズレ量が非常に大きいケースでは，感覚性および運動性の融像が低値を示していた．

結論：顕微鏡下での奥行き感の精度には，両眼視機能が影響することが示唆された．今回試作したM三杆法は，まだ開発段階ではあるが，顕微鏡下作業の適正判定の一助となる可能性が示された．

【キーワード】 顕微鏡，両眼視機能，三杆法，融像，立体視

緒言

眼科領域では細隙灯顕微鏡や手術用顕微鏡などの光学顕微鏡が汎用されている[1]．また，精密器械の技術者や，生命科学の研究者も双眼顕微鏡を使用する機会が多い．その中には，日常視下では立体視が良好であるにもかかわらず，顕微鏡下では立体視ができずに複視を感じる者や，奥行きの判断が困難な者がいる．

今回我々は，M三杆法装置を試作し，顕微鏡下で立体感を得られにくいケースの要因を検討する目的で，顕微鏡下と非顕微鏡下での両眼視機能につき比較検討を行ったので報告する．

対象および方法

1．対象

眼疾患がなく，正常な視力とTSTのcirclesで40秒の立体視が認められた33例(男性11例，女性22例)で，年齢は22～44(平均29.6±4.9)歳であった．屈折異常が大きいほうの眼の屈折は等価球面値で＋0.75～－8.5(平均－1.2±1.7) D，乱視が1.5D以上あったのは4眼2例(－2.25D，－3.25D)，不同視差が2.0D以上あったのは2例(1.5D，2.5D)であった．眼位は正位または外斜位で，交

1 大阪大学医学部感覚器外科学講科 Department of Ophthalmology, Osaka University Graduate School of Medicine
2 医療法人明和病院 Meiwa Hospital
3 大阪府立急性期・総合医療センター Osaka General Medical Center
4 財団法人日本生命済生会付属日生病院 Nissay Hospital
5 大阪大学医学部感覚器機能形成学教室 Department of Applied Visual Science, Osaka University Graduate School of Medicine

＊別刷請求先 565-0871 大阪府吹田市山田丘2-2
大阪大学医学部感覚器外科学講科 平井教子

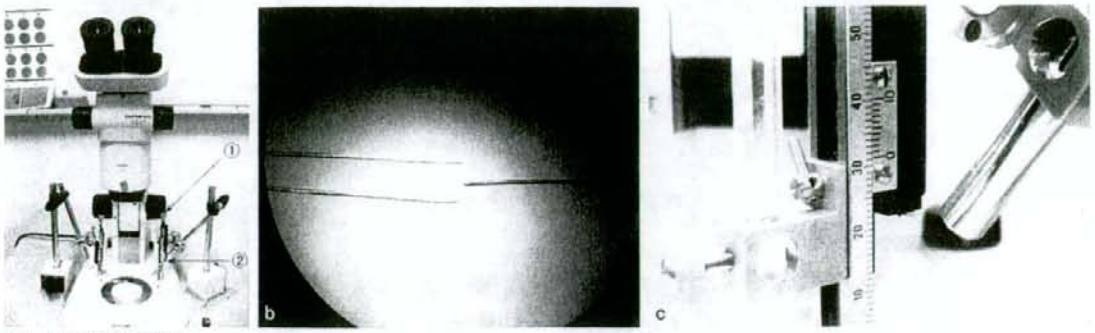

図1　M三杆法について
a：全景写真．①つまみ（被検者自身で回してもらうと三杆部分の一本の棒が上下する），②マイクロメーター．b：三杆部分の実際の見え方．c：マイクロメーター部の拡大．

代プリズム遮閉試験による遠見斜視角は，+2～−14（平均−3.7±3.3）⊿であった．

2．検査装置

（1）M三杆法

ガリレオ式平行光学系の顕微鏡（OLYMPUS社）の対物レンズの下方に，マニピュレータ（Narishige，BE-806009）に針金（直径0.5mm，長さ50mm）を取り付けたものを設置し，M三杆法装置を作成した（**図1a**）．顕微鏡を覗くと，視野には左側に2本の棒，右側に1本の棒が見える（**図1b**）．左側の2本の棒は定位置で固定しており，右側の1本の棒をつまみ操作により下から上へと被検者自身で動かしてもらい，3本の棒が同じ高さになったと自覚した時点でつまみ操作を終了させ，左側の2本の棒とのズレ量を測定する．ズレ量は，マイクロメーターにより0.1mmの精度での評価が可能である（**図1c**）．顕微鏡の倍率は2倍で行い，5回測定の平均値（絶対値）を算出した．測定に先立って，被検者には検査に慣れてもらう目的で，十分に視度と瞳孔間距離を調整した上で何度か練習してもらい，測定時には，反復せずに下から上への一方向のみに動かしてもらった．

（2）細隙灯顕微鏡（スリットランプ）

用いたスリットランプ（カールツァイスメディテック社製）は，平行光学系の器械であり，5倍の拡大下で測定を行った[2]．

3．方法

顕微鏡下での検査として，M三杆法を両眼視下と片眼視下で測定し，加えてスリットランプ下でTSTのcirclesを施行した．

非顕微鏡下での検査として，TNO，ワック社製のD' ACOMOにより調節幅を，さらに大型弱視鏡による融像幅とAC/A比を測定した．以上の検査はすべて完全矯正下で施行し，それぞれの検査結果の比較検討を行った．

4．統計処理

paired t-test，およびSpearman rank order correlationで統計学的検討を行い，$p \leqq 0.05$を有意とみなした．

結果

最初に，M三杆法における両眼視下と片眼視下でのズレ量の比較を行った（**図2**）．ズレ量は，両眼視下で0.9±0.99mm，片眼視下で4.42±4.23mmであり，M三杆法におけるズレ量は，片眼視下と比較して両眼視下で有意に少なかった（$p < 0.001$，paired t-test）．

次に，スリットランプ下でのTSTとM三杆法の比較を示す（**図3**）．M三杆法でのズレ量が小さい場合，スリットランプ下でのTSTも小さな視差まで正答可能な人が多く，またM三杆法でのズレ量が大きい場合，スリットランプ下でのTSTでも大きな視差でしか正答できない人が存在したが両者に有意な関係はみられなかった（$r = -0.205$，$p = 0.249$，Spearman）．

TNOとM三杆法の比較においては（**図4**），M三杆法でのズレ量が小さいケースではTNOの成績も良好であり，ズレ量が大きいケースではTNOの成績が低値を示し，両者は有意に相関した（$r = -0.390$，$p = 0.0253$，Spearman rank order correlation）．

調節幅とM三杆法の比較では（**図5**），M三杆法のズレ量が小さいケースでも調節幅にバラつきがあり，有意ではなかったが融像幅が狭いとM三杆法の値は大きくなる傾向があった（$r = -0.313$，$p = 0.0762$，Spearman rank order correlation）．

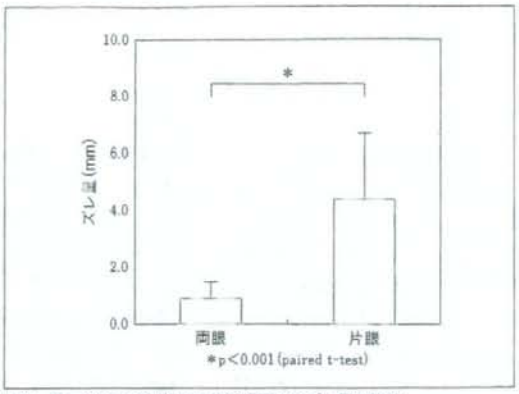

図2　M三杆法の両眼視下と片眼視下でのズレ量の比較
M三杆法におけるズレ量は，片眼視下と比較して両眼視下で有意に少なかった．

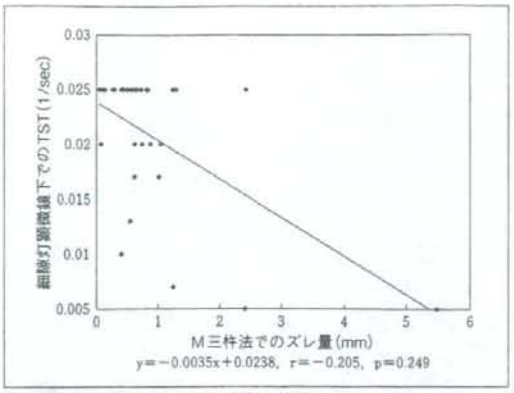

図3　顕微鏡下でのTSTとM三杆法の比較
縦軸の視差の目盛りは，秒の逆数で表しており，目盛りの数値が大きいほど視差は小さくなる．M三杆法とスリットランプ下でのTSTに有意な関係はみられなかった．

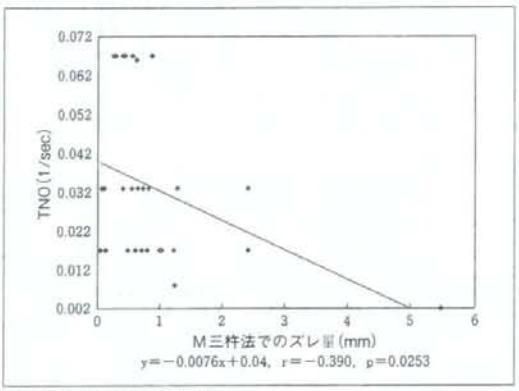

図4　TNOとM三杆法の比較
TNOとM三杆法の結果は有意に相関した．

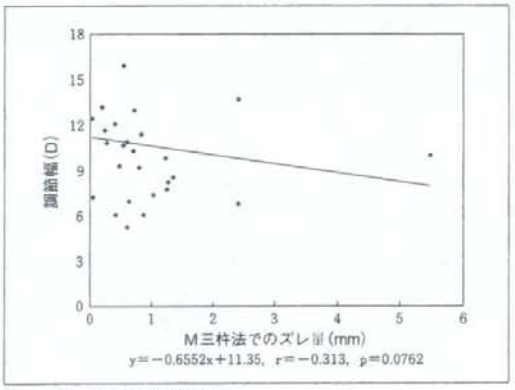

図5　調節幅とM三杆法の比較
調節幅にバラつきはあるが，統計的には有意ではなかった．

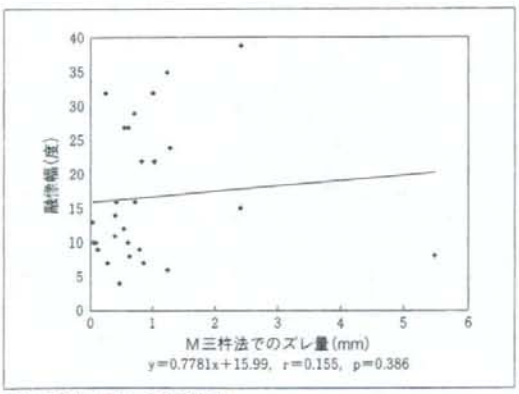

図6　融像幅とM三杆法の比較
広い範囲にバラつきがみられたが，有意な相関は認められなかった．

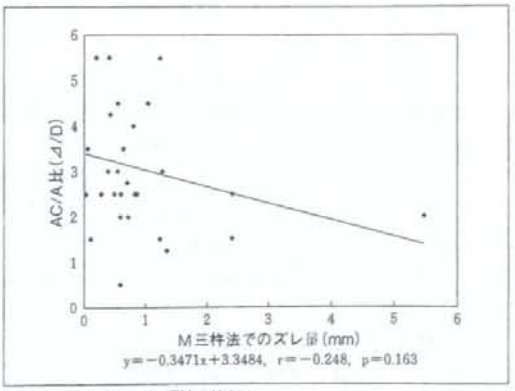

図7　AC/A比とM三杆法の比較
M三杆法のズレが大きい人はAC/A比が小さい傾向があったが，有意な相関は認められなかった．

融像幅とM三杆法の比較(図6)，AC/A比とM三杆法の比較(図7)においては，M三杆法のズレ量が小さい人でも，融像幅やAC/A比に広い範囲でバラつきがみられ，有意な相関は認められなかった($r=0.155$, $p=0.386$, $r=-0.248$, $p=0.163$, Spearman)．

最後に，M三杆法のズレ量が最も大きかった1例の各検査における成績を検討する．各グラフでM三杆法のズレ量が5.6mmの症例であるが，25歳の男性で屈折が−0.88D，眼位は−2⊿であった．スリットランプ下のTST，TNO，融像幅がすべて低値を示していた．被検者にM三杆法の感想を聞くと，両眼視下ではあったが，三杆の中央の棒が上下しているのがわからなかったと述べている．

考按

一般的に，両眼を分離して立体的にものを見る装置では眼精疲労をきたしやすく，その原因として，機器の幾何学的な特性や輻湊と調節の矛盾等が挙げられている[3]．また，画質や奥行きの調整など機器側の光学系の設定の問題や，調節や使用環境など被検者側の条件に原因があるともいわれている[4]．

今回我々が試作した三杆法装置は，眼科で普及している細隙灯顕微鏡に類似した低倍率の実体顕微鏡(ガリレオ式の平行光学系のもの)下で，三杆法を行うものであり(図1)，測定は十分に視度と瞳孔間距離を調整した上で行った．その結果，片眼視時と比較して両眼視時のほうが有意にズレ量が少なかった(図2)．このことから，顕微鏡下で奥行き感の同定をするには両眼視が必要であり，両眼視機能が奥行き感の精度に影響することが示唆された．また同時に，開発したM三杆法装置の有用性を確認することができた．

今回の対象者は全員非顕微鏡下ではTSTで40秒の立体視機能が認められていたが，スリットランプ下でTSTを行った結果は，ばらつきがみられ，両眼分離が強い条件では，TSTが正常範囲にあっても，立体視が低下することが確認された(図3)．M三杆法とスリットランプ下でのTSTの結果には有意な相関はみられなかったが，M三杆法と，非顕微鏡下のTNOの結果には有意な相関がみられた．

M三杆法は，両眼分離下で主として調節および視差の手がかりを基に立体視を調べる検査といえる．TNOは赤緑眼鏡を用いて，比較的強い両眼分離下で精密な立体視を調べる検査である．両者は，強い両眼分離下での精密な両眼視機能が必要な検査という点が共通しているため，有意な相関がみられたのではないかと考えられた．また，TNOの方がTSTより小さい視差まで測定可能であることも，有意な相関が得られた一因と考えられた．

M三杆法の成績が悪かった被検者では，顕微鏡下でのTSTや非顕微鏡下でのTNO，融像幅といった感覚性および運動性の融像が不良であった．実際その被検者は顕微鏡を使用し始めた当初は，顕微鏡下での両眼視に違和感があり1ヵ月の間は立体視ができなかったと述べている．手術用顕微鏡下では非顕微鏡下と比較して立体視能力が低下するという報告がある[5]．一方，顕微鏡では左右の像が分離しており，像がとまっている場合には精密な立体視が必要と考えられるが，実際の顕微鏡下の操作は器具を動かして行うため，影や輪郭の重なりなどが奥行き感覚の手掛かりとなり，経験を積めば視差に依存した立体視が弱くとも十分作業が行える[6]，という報告もある．今回のM三杆法の成績が悪かったケースはこれに該当しており，実際に，1ヵ月後は顕微鏡下での作業に支障がなくなっている．経験を積むことにより顕微鏡下での作業が可能になった一例であると考えられた．

今回試作したM三杆法は，まだ開発段階ではあるが，顕微鏡下作業の適正判定の一助となる可能性が示された．今後は，融像能力が弱い斜視や弱視の症例を対象に，さらに検討を行う予定である．

文献

1) 魚里　博：顕微鏡光学に関する基礎知識．野田　徹(編)：眼科診療プラクティス97　細隙灯顕微鏡のすべて．文光堂，東京，98-102，2003.
2) 野田　徹：顕微灯顕微鏡の基本構造．野田　徹(編)：眼科診療プラクティス97　細隙灯顕微鏡のすべて　文光堂，東京，102-107，2003.
3) 矢野澄男，井出真司，他：立体画像の見やすさと調節応答からみた視覚疲労　映像情報メディア学会誌 55：711-717，2001.
4) 山内康司，篠原一彦：立体内視鏡下手術操作時の疲労に対する両眼立体視の影響．J JSCAS 7：115-125，2005.
5) Du LT, Wessels IF, et al：Stereoacuity and depth perception decrease with increased instrument magnification comparing a non-magnified system with lens loupes and a surgical microscope. Binocul Vis Strabismus Q 16：61-67, 2001.
6) 不二門尚，田野保雄：日常視に必要な立体視に関する臨床的考察－周辺網膜における両眼視機能の役割－．眼紀 45：857-861，1994.

Jpn J Ophthalmol 2008;52:380–385
© Japanese Ophthalmological Society 2008

DOI 10.1007/s10384-008-0575-1

CLINICAL INVESTIGATION

Photoreceptor Images of Normal Eyes and of Eyes with Macular Dystrophy Obtained In Vivo with an Adaptive Optics Fundus Camera

Kenichiro Bessho[1], Takashi Fujikado[1], Toshifumi Mihashi[2], Tatsuya Yamaguchi[2], Naoki Nakazawa[2], and Yasuo Tano[3]

[1]Applied Visual Sciences, Osaka University Graduate School of Medicine, Osaka, Japan; [2]Topcon Corporation Inc., Tokyo, Japan; [3]Department of Ophthalmology, Osaka University, Graduate School of Medicine, Osaka, Japan

Abstract

Purpose: To report on images of the human photoreceptor mosaic acquired in vivo with a newly developed, compact adaptive optics (AO) fundus camera.

Methods: The photoreceptors of two normal subjects and a patient with macular dystrophy were examined by using an AO fundus camera equipped with a liquid crystal phase modulator. In the eye with macular dystrophy, the fixation point in the AO images was identified using scanning laser ophthalmoscope (SLO) microperimetric image superimposed on a color fundus photograph.

Results: Photoreceptor cells were detected as bright dots approximately 4 μm in diameter in normal subjects. In the eye with macular dystrophy, the fixation point was located within the bull's eye lesion and uniform small whitish spots with irregular patchiness were observed in the AO images of this area. The distance between the small spots was 3–4 μm. In other parts of the bull's eye retinal lesion, the whitish spots were larger and of different sizes.

Conclusions: The photoreceptor mosaic could be identified in photographs of eyes of normal subjects and an eye with macular dystrophy in vivo by an AO fundus camera. In the eye with macular dystrophy, a relatively uniform photoreceptor mosaic was observed around the fixation point, whereas presumed debris of photoreceptor degradation was observed in the other bull's eye retinal lesion. **Jpn J Ophthalmol** 2008;52:380–385 © Japanese Ophthalmological Society 2008

Key Words: adaptive optics, cone mosaic, macular dystrophy, retinal imaging

Introduction

Adaptive optics (AO) technology, originally developed by astronomers to use with ground telescopes to compensate for atmospheric turbulence, has now been applied to fundus imaging. AO increases the resolution limits of retinal images by compensating for ocular wavefront aberrations.[1,2] Using an AO device, several studies have reported in vivo imaging of normal retinas[2–6] and the two-dimensional configuration of cone mosaic images. Recently, photoreceptor images from eyes with macular dystrophy have been obtained,[7,8] and a decrease of cone density was observed, which was correlated with a decrease in the amplitude of multifocal electroretinograms (ERGs). However, none of these reports referred to the fixation area in relation to the cone mosaic images.

The AO system consists of a wavefront sensor and a wavefront corrector, which form a closed loop of real-time wavefront compensation. The optical image with a reduced wavefront error is transferred to an imaging device such as a confocal scanning laser ophthalmoscope (SLO),[3] an optical coherence tomograph,[4] or a conventional fundus

Received: November 5, 2007 / Accepted: June 3, 2008

Correspondence and reprint requests to: Takashi Fujikado, Department of Applied Visual Sciences, Osaka University Graduate School of Medicine, 2-2 Yamadaoka, Suita, Osaka 565-0871, Japan
e-mail: fujikado@ophthal.med.osaka-u.ac.jp

camera.[1,2,5] The combination of a Hartmann-Shack wavefront sensor and a mechanical deformable mirror wavefront corrector seems to be the most widely used current AO system.

We developed a compact AO fundus camera using a Hartmann-Shack sensor and a liquid crystal wavefront modulator. We reported previously that our system could resolve individual photoreceptors in healthy eyes, and we have now used this system to measure interphotoreceptor spacing in both normal eyes and myopic eyes.[9]

Here we report another way in which our AO system can be applied. Our aim was to compare the AO images of a normal retina with those of an eye with macular dystrophy. More specifically, we examined whether the configuration of the cone mosaic in the fixation area differed from that in other areas within a bull's eye lesion.

Methods

Adaptive Optics System

A schematic diagram of the AO system is shown in Fig. 1. The main components of the system are a nematic liquid crystal phase modulator (LCPM; X8267-12, Hamamatsu Photonics, Hamamatsu, Japan), a Hartmann-Shack wavefront sensor (HSWS; 28 × 28 lenslets, especially made by Topcon, Tokyo, Japan), and a scientific charge-coupled device (CCD) digital camera (C9100-02, Hamamatsu Photonics). The light source for the wavefront sensing path was a 690-nm super luminescence diode (FiberMax, Blue Sky Research, Milpitas, CA, USA), and that for the retinal illumination path was a 635-nm laser diode (LLS-635–50, Moritex, Tokyo, Japan).

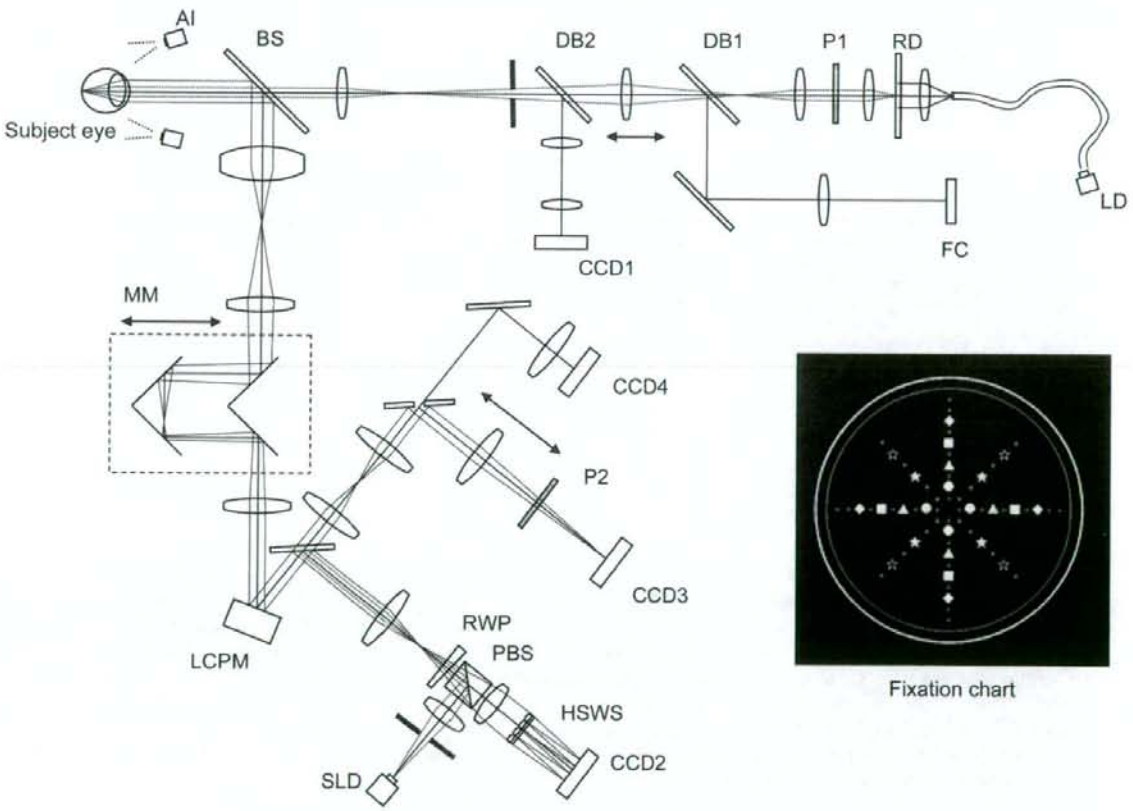

Figure 1. Schematic diagram of an adaptive optics fundus camera using a liquid crystal light modulator. AI, light source (LED 940 nm) for anterior segment illumination; *LD*, laser diode illuminator (635 nm); *SLD*, super luminescence diode illuminator (690 nm); *CCD*, charge-coupled device; *BS*, beam splitter; *DB1/DB2*, dichroic beam splitter; *FC*, fixation chart; *RD*, rotating diffuser; *P1*, *P2*, linear polarizers; *MM*, moving mirror; *RWP*, rotary wedged prism; *HSWS*, Hartmann-Shack wavefront sensor; *LCPM*, liquid crystal phase modulator (Hamamatsu PAL-SLM).

Jpn J Ophthalmol
Vol 52: 380–385, 2008

To avoid generation of speckles due to the coherence of the light sources, a rotary wedged prism was placed in the optical path of the HSWS, and a light-shaping diffuser sheet (LSD, Physical Optics, Torrance, CA, USA), which rotated at 20000 rpm in the retinal illumination path.

The HSWS measured the ocular wavefront up to the eighth Zernike order, and the LCPM compensated for the measured wavefronts. These two components formed a closed loop of continuous wavefront compensations, and operated at approximately 3 Hz, limited by the working speed of the LCPM. The system was also equipped with coaxial, 8° wide view optics to identify the location and orientation of the highly magnified retinal images observed. The area occupied by the AO system was 0.8 m × 0.8 m with a height of 25 cm, which might be compact enough to place in a clinical examination room. The entire AO system can be maneuvered by a single operator. Each series of AO images from the selected retinal locus can be captured in about 2 min, including targeting of the area, focusing, and wavefront compensation.

Subjects

A 40-year-old Japanese man presented with a progressive decrease of visual acuity over 20 years; his best-corrected visual acuity was 20/60 OU. Ophthalmoscopic examination revealed an annular zone of retinal pigment epithelial atrophy in the macula (bull's eye maculopathy) in both eyes (Fig. 2). His younger brother had a similar macular lesion. Bilateral ring scotomas were detected in both eyes of the patient by Goldmann perimetry. A moderate window defect without leakage was observed in the macular area by fluorescein angiography. The 30-Hz flicker ERGs and flash ERGs were of normal amplitude.

Two healthy volunteers (a 38-year-old man and a 31-year-old woman) were also examined.

Image Capturing

The research protocols were approved by the institutional review board of Osaka University Medical School and conformed to the tenets of the Declaration of Helsinki. After the nature and possible consequences of the study were explained, written informed consent was obtained from the two subjects and the patient.

After the pupils were dilated by topical 0.5% tropicamide and 0.5% phenylephrine, the examinee was seated in front of the AO system with a regular chin rest and asked to fixate the target. A retinal photograph was taken by the CCD as a 20-frame movie sequence with 10-bit grayscale images (1000 × 1000 pixels) and the total root mean square (RMS) error was reduced below the preset trigger value (usually 0.10 μm for a 5-mm pupil). The magnification of the image was calculated from the axial length of the eye.[10]

In the macular dystrophy patient, the retinal locus of fixation was verified by microperimetry using a confocal SLO (Rodenstock SLO ver 1.0, Rodenstock, Munich, Germany),[11] conventional color fundus photographs (Topcon TRC50LX, Topcon), and optical coherence tomography (OCT3000, Carl Zeiss Meditec, Dublin, CA, USA). The mosaic AO image was manually processed with Adobe Photoshop CS1 (Adobe, San Jose, CA, USA) image-processing software. With the same software, the color fundus image and the SLO image were superimposed on the mosaic AO image and the retinal locus of fixation in the AO image was determined.

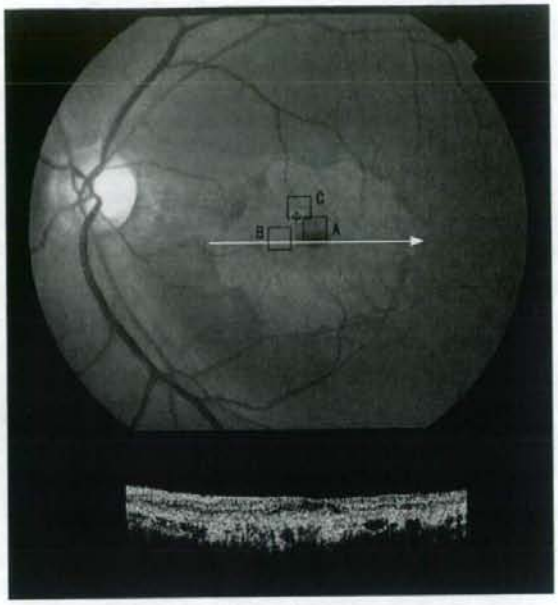

Figure 2. Fundus and optical coherence tomography (OCT) images of the left eye of a patient with macular dystrophy. The *blue cross* represents the fixation point, verified by the scanning laser ophthalmoscope microperimetry. The *white arrow* shows the position of the OCT transect. The *square boxes* represent the areas examined by adaptive optics (AO) and are labeled with *letters* corresponding to the parts of Fig. 4.

Calculation of the Cone Density

Cone density was calculated in three steps.

1. Image processing of each grabbed image before image summation using the deconvolution function, "deconvlucy," of MATLAB (Mathworks, Natick, MA, USA) was performed to get a clear separation of the cones.
2. Image summation to improve the signal-to-noise ratio was performed using our original program. The number of superimposed images ranged from 8 to 64 frames, depending on the imaging conditions.
3. The cones were marked. Retinal loci about 2° temporal of the center of the fovea were examined. Three 100 μm

× 80 μm rectangular areas were selected, excluding those in which retinal vessels had a cone mosaic that required degrading. Bright spots 2–5 μm in diameter were considered to be cones. A single examiner (KB) manually marked the cones in the target area. The examiner used the accented edges function of Photoshop CS1 whenever this function made the task easier. However, even when this function was used, the final identification of the cone was always done by observing the original averaged image.

Results

In both the volunteers and the patient, the ocular aberration was reduced to below 0.1 μm RMS (Table 1). In the two normal subjects, the photoreceptors were imaged as slightly oval-shaped bright dots with a tiled packing arrangement (Fig. 3; the AO image of normal subject 2 is not shown). The diameter of the bright dot was approximately 4 μm, and the density was 40950/mm^2 and 54530/mm^2 at 2° from the fovea centralis. These values are comparable to those obtained by another histological study of the human cone mosaic (40000–50000/mm^2).[12]

In the eye with macular dystrophy, the visual field obtained by the SLO microperimetry showed a ring scotoma. The fixation point was located within the bull's eye lesion and was approximately 200 μm superonasal from a central dark area (Fig. 2). The OCT images showed cystic changes in the fovea and degenerative changes of the retinal pigment epithelium in the macular area, but the precise degree of photoreceptor degeneration could not be determined.

In the AO retinal image, the observed morphology of the photoreceptor layer varied considerably, suggesting degeneration of the photoreceptors (Fig. 4). No structure was observed in the central dark area, and the shape of the white dots in the surrounding bright-colored area varied widely (Fig. 4A). Relatively uniform white dots were observed at several loci in the same area.

In the area where the white dots were uniformly distributed, the distance between spots was 3–4 μm, comparable

Table 1. Profiles of subjects

	Normal 1	Normal 2	Patient
Sex	Male	Female	Male
Age (years)	38	31	40
Imaged eye	OS	OS	OS
Retinal status	No disease	No disease	Macular dystrophy
BCVA	20/15	20/20	20/60
Subjective refraction	Sph-1.0 D	Sph-0.9 D	Sph-1.8 D
	Cyl-0.3 D	Cyl-0.2 D	Cyl-0.8 D
RMS[a] without AO (μm)	0.317	0.213	0.306
RMS with AO (μm)	0.083	0.078	0.094
Average cone density[b] (cones/mm^2)	40950	54530	ND

BCVA, best-corrected visual acuity; RMS, root mean square; AO, adaptive optics; ND, not done.

[a]Root mean square value of aberration coefficients of the second to eighth Zernike order for a 5-mm pupil diameter. The 2° temporal from the fovea was measured.

[b]Calculated from the cone spacing in the area 2° temporal from the fovea.

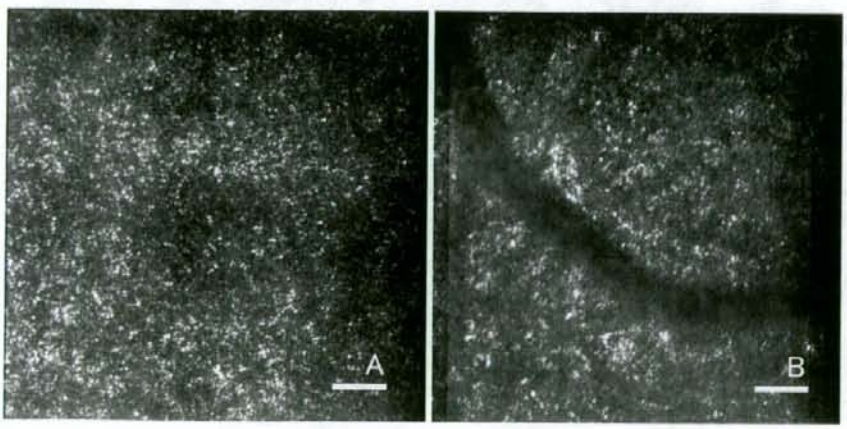

Figure 3A, B. AO image of a normal subject. Deconvolution was performed by using residual wavefront error data and subsequently five frames were averaged. **A** Center of the macula. The image covers the foveal avascular zone. The foveal center appears relatively darker than the surrounding area. **B** Three degrees temporal to the foveal center. Bar = 50 μm.

Jpn J Ophthalmol
Vol 52: 380–385, 2008

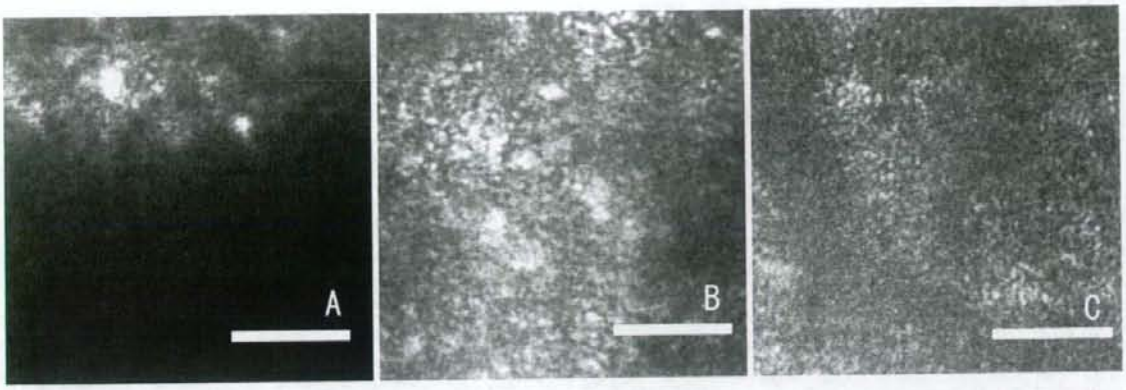

Figure 4A–C. Individual AO images of the sampled areas. The orientation of each image was determined by creating a composite AO image and registering it on the color fundus picture in Fig. 2. The letters correspond to the labeled sampling areas in Fig. 2. The total residual root mean square wavefront error was 0.089, 0.090, 0.162 μm for **A–C**, respectively, for a 5-mm pupil. **A** Upper edge of the central dark area. Very large irregular spots are seen above the dark area. **B** Example of an image with large, scattered, irregular spots. **C** Area near the locus of fixation. The dark vertical streak represents a capillary vessel. A patchy dark area is also seen on the right side of the image. Bar = 50 μm.

to that in the normal eyes and consistent with the interphotoreceptor distance obtained from histological data.[12]

In the nonuniform area, the bright spots were larger, ranging from 2 to 20 μm, and less uniform than those in the normal retinas, in which photoreceptors appeared as uniform small spots of 2–5 μm (Fig. 4B).[12] In the fixation area, the spots were more uniform in size and the overall appearance was more similar to normal retinas (Fig. 4C).

Discussion

The AO system used in this study is equipped with an LCPM as a wavefront corrector instead of the deformable mirror used in other AO systems. In our previous study we showed that this compact AO system can still effectively resolve cone photoreceptors. On the other hand, the LCPM has several limitations. The current system operates at approximately 3 Hz; thus, eye movement can affect the image quality. In this study, all subjects, including the macular dystrophy patient, had good fixation as judged from the AO images in the movie sequence, so the eye movement may not have been significant. We selected a 690-nm laser diode as the illuminator in order to reduce glare during the examinations. Because the coherence of this illuminator causes speckles, we used a rotating diffuser. Another problem may be that the LCPM can modulate only polarized light. This means that with this system we could obtain only partial optical information from the retina, which might be a problem when precise optical properties of retinal microstructures are studied, but we believe that the system is still applicable to the study of two-dimensional photoreceptor arrangements or photoreceptor morphology.

In the normal subjects, it was possible to obtain clear images of the photoreceptors with good wavefront compensation (Fig. 2). In this study, the calculated size of each spot was 2–5 μm, consistent with that obtained by other studies using a high-resolution system[13] or OCT[14] and by histological studies.[12]

In the eye with macular dystrophy, several patterns of AO image were seen in the bull's eye lesion. A central dark-colored area was uniform without structure. This may indicate either that a disorder of the inner retinal layers blocked the image or that the photoreceptors in this area are absent.

In the surrounding rough bright-colored area, scattered white spots of different shapes and sizes were seen. As this area showed reduced retinal sensitivity in SLO microperimetry, these spots may represent either morphologically changed photoreceptors or photoreceptor degeneration debris (Fig. 4).[8]

The fixation point on the retina was also located in the surrounding rough bright-colored area. The AO image showed a rather uniform distribution of white spots whose separation was consistent with the cone mosaic. It is possible that the photoreceptors were less affected in the fixation area.

The image obtained using the AO system is not fully understood. The spots in the AO images might be inner segment–outer segment (IS/OS) photoreceptor junctions because in the normal retina each spot seems to be in a one-to-one correspondence with a single photoreceptor, and because recent studies using high-resolution OCT suggest that the IS/OS junction seems to show its highest reflectivity inside the photoreceptor layer.[15] At the same time, it has been observed that this IS/OS reflection tends to disappear and reappear during the course of retinal diseases such as serous macular detachment[16] or macular hole, indicating that the IS/OS reflection probably indicates a functional aspect of the photoreceptors and that loss of the IS/OS reflection does not necessarily mean the absence of

the photoreceptor itself. Considering this, we note that the absence of regular spots does not necessarily mean the absence of photoreceptors, but it may indicate a functional change in the photoreceptors. In the same way, irregular spots, too, may be signs of a functional change in the photoreceptors. It may be possible to learn more about this issue by a study combining AO fundus camera and high-resolution OCT images.

Although our AO system has several limitations, we have shown that a two-dimensional image of photoreceptor cells can be obtained that is useful for examining macular dystrophy. In the future, animal studies are needed to investigate the origin of the large spots, and studies to improve the resolution of the AO system for quantitative evaluation of residual photoreceptors in diseased retinas are also needed.

Acknowledgments. Kenichiro Bessho and Takashi Fujikado had full access to all data in the study and take responsibility for the integrity of the data and the accuracy of the data analysis. This study was supported by a Health Sciences Research Grant (H19-sensory-001) from the Ministry of Health, Labour and Welfare, Japan

References

1. Liang J, Williams DR, Miller DT. Supernormal vision and high-resolution retinal imaging through adaptive optics. J Opt Soc Am A 1997;14:2884–2892.
2. Roorda A, Williams DR. The arrangement of the three cone classes in the living human eye. Nature 1999;397:520–522.
3. Roorda A, Romero-Borja F, Donnelly WJ III, et al. Adaptive optics scanning laser ophthalmoscopy. Opt Express 2002;10: 405–412.
4. Hermann B, Fernandez EJ, Unterhuber A, et al. Adaptive-optics ultrahigh-resolution optical coherence tomography. Opt Lett 2004;29:2142–2144.
5. Doble N, Yoon G, Chen L, et al. Use of a microelectromechanical mirror for adaptive optics in the human eye. Opt Lett 2002;27: 1537–1539.
6. Roorda A, Metha AB, Lennie P, Williams DR. Packing arrangement of the three cone classes in primate retina. Vision Res 2001;41:1291–1306.
7. Wolfing JI, Chung M, Carroll J, et al. High-resolution retinal imaging of cone-rod dystrophy. Ophthalmology 2006;113: 1014–1019.
8. Choi SS, Doble N, Hardy JL, et al. In vivo imaging of the photoreceptor mosaic in retinal dystrophies and correlations with visual function. Invest Ophthalmol Vis Sci 2006;47:2080–2092.
9. Kitaguchi Y, Bessho K, Yamaguchi T, et al. In vivo measurements of cone photoreceptor spacing in myopic eyes from images obtained by an adaptive optics fundus camera. Jpn J Ophthalmol 2007;51: 456–461.
10. Bennett AG, Rudnicka AR, Edgar DF. Improvements on Littmann's method of determining the size of retinal features by fundus photography. Graefes Arch Clin Exp Ophthalmol 1994;232: 361–367.
11. Oyagi T, Fujikado T, Hosohata J, et al. Foveal sensitivity and fixation stability before and after macular translocation with 360-degree retinotomy. Retina 2004;24:548–555.
12. Curcio CA, Sloan KR, Kalina RE, Hendrickson AE. Human photoreceptor topography. J Comp Neurol 1990;292:497–523.
13. Miller DT, Williams DR, Morris GM, Liang J. Images of cone photoreceptors in the living human eye. Vision Res 1996;36: 1067–1079.
14. Pircher M, Baumann B, Gotzinger E, Hitzenberger CK. Retinal cone mosaic imaged with transverse scanning optical coherence tomography. Opt Lett 2006;31:1821–1823.
15. Zawadzki RJ, Choi SS, Jones SM, et al. Adaptive optics-optical coherence tomography: optimizing visualization of microscopic retinal structures in three dimensions. J Opt Soc Am A Opt Image Sci Vis 2007;24:1373–1383.
16. Ojima Y, Hangai M, Sasahara M, et al. Three-dimensional imaging of the foveal photoreceptor layer in central serous chorioretinopathy using high-speed optical coherence tomography. Ophthalmology 2007;114:2197–2207.

Jpn J Ophthalmol 2008;52:386–392
© Japanese Ophthalmological Society 2008

DOI 10.1007/s10384-008-0568-0

LABORATORY INVESTIGATION

Changes in Muscle Fiber Size and in the Composition of Myosin Heavy Chain Isoforms of Rabbit Extraocular Rectus Muscle Following Recession Surgery

Sung Chul Park, Yun Taek Kim, Sun A Kim, and Sei Yeul Oh

Department of Ophthalmology, Samsung Medical Center, Sungkyunkwan University School of Medicine, Seoul, Republic of Korea

Abstract

Purpose: To assess the changes in the size of muscle fibers and the composition of myosin heavy chain (MyHC) isoforms in the global layer (GL) and the orbital layer (OL) of rabbit rectus extraocular muscle (EOM) after recession.

Methods: The right superior rectus muscles of two rabbits were harvested at 3 days or 1, 2, or 4 weeks after recession (eight rabbits in total). At each time point, one muscle was used for measuring the cross-sectional area of the muscle fibers and the other for identifying the composition of MyHC. The right superior rectus muscles of three additional naïve rabbits were used as controls.

Results: The mean cross-sectional area of the OL fibers did not change significantly. However, that of the GL fibers significantly decreased at 3 days ($P < 0.001$) and 1 week ($P = 0.024$) postoperatively, and increased thereafter to reach the control levels at 2 and 4 weeks postoperatively. Three days after surgery, the total MyHC content and the proportion of type IIb MyHC (MyHCIIb) plus EOM-specific MyHC (MyHCeom) decreased and remained at its lower level for 4 weeks.

Conclusions: Transient atrophy and regeneration were observed only in the GL, and the changes in the MyHCIIb plus MyHCeom appeared to be related to these changes. **Jpn J Ophthalmol** 2008;52:386–392
© Japanese Ophthalmological Society 2008

Key Words: extraocular muscle, global layer, myosin heavy chain, orbital layer, recession

Introduction

The extraocular muscles (EOMs) are unique skeletal muscles that perform highly coordinated and complex movements such as fast saccades, smooth slow pursuit and vergence movements, and fixation on a given position. The EOMs can be divided into two distinct parts, the orbital layer (OL) and the global layer (GL).[1–3] The OL lies along the EOM surface facing the orbital wall, and the GL faces the eyeball and is partially enclosed by the OL. The active pulley hypothesis suggests that the GL and the OL have distinctive roles in ocular motility.[4–6] The GL terminates at the myotendinous scleral insertion and acts directly on the globe to move the eye, whereas the OL branches off further posteriorly and penetrates a sheath of connective tissue that acts as a pulley controlling the plane of eye rotation.[4–6]

Myosin is the major contractile protein in skeletal muscles, and the relative myosin isoform composition determines the contractile and biochemical properties of each skeletal muscle.[7] Myosin heavy chain (MyHC) contains adenosine triphosphatase and an actin-binding site, and is believed to have the largest effect on the speed of contraction, contractility, and fatigue resistance of skeletal

Received: November 23, 2007 / Accepted: June 1, 2008
Correspondence and reprint requests to: Sei Yeul Oh, Department of Ophthalmology, Samsung Medical Center, Sungkyunkwan University School of Medicine, 50 Ilwon-dong, Kangnam-ku, Seoul 135-710, Republic of Korea
e-mail: syoh@skku.edu

Adaptive Optics Fundus Camera to Examine Localized Changes in the Photoreceptor Layer of the Fovea

Yoshiyuki Kitaguchi, MD,[1] Takashi Fujikado, MD,[1] Kenichiro Bessho, MD,[1] Hirokazu Sakaguchi, MD,[2] Fumi Gomi, MD,[2] Tatsuo Yamaguchi, MS,[3] Naoki Nakazawa, BE,[3] Toshifumi Mihashi, PhD,[3] Yasuo Tano, MD[2]

Purpose: To examine highly localized photoreceptor disruptions in the fovea by a high-resolution adaptive optics (AO) fundus camera combined with Fourier-domain optical coherence tomography (FD OCT).

Design: Observational case series.

Participants: Three eyes of 3 patients who showed dark foveal spots by slit-lamp biomicroscopy.

Methods: Three patients who reported metamorphopsia but showed no changes in the retina in conventional fundus photographs were examined. High-resolution retinal images were obtained with the AO fundus camera and by FD OCT. The images were compared with the findings obtained by standard clinical tests, including Amsler charts and fluorescein angiography (FA).

Main Outcome Measures: Quantitative measurements of the area of photoreceptor disruption.

Results: Slit-lamp biomicroscopy revealed an irregularly shaped dark spot in the fovea centralis but no changes in FA in the 3 cases. The photoreceptor mosaic was absent in a highly localized area of the fovea in the images obtained by the AO fundus camera, and the photoreceptor outer segment was absent or disturbed at the corresponding area by FD OCT in all 3 cases. The horizontal and vertical sizes of the area of disturbance of the photoreceptor mosaic in the AO images in the 3 eyes were 400×200 μm, 300×120 μm, and 300×200 μm. These sizes were comparable to the photoreceptor outer segment disturbances in the OCT images which were 330×150 μm, 280×100 μm, 200×150 μm, respectively.

Conclusions: Localized OS disturbances were able to be detected in eyes with a dark foveal spot by AO fundus camera 2-dimensionally and by FD OCT axially. The good correspondence of the sizes of the area of photoreceptor disturbances obtained by AO images to those by FD OCT images indicate that the AO images can be used to evaluate and follow the 2-dimensional area of focal changes of the photoreceptors in the fovea quantitatively.

Financial Disclosure(s): Proprietary or commercial disclosure may be found after the references.
Ophthalmology 2008;115:1771–1777 © 2008 by the American Academy of Ophthalmology.

With current advanced retinal imaging instruments, small focal changes of the retina can be detected and measured more accurately. These findings can help in determining the cause of unexplained visual symptoms and visual loss. For example, the retina of patients at the early phase of macular dystrophy appears ophthalmoscopically normal.[1–6] However, examination of optical coherence tomography (OCT) images showed that the retina was thinner at the macular area and that the decrease in thickness was correlated with the reduced visual acuity.[4] With additional improvements in the axial resolution by ultra–high-resolution OCT, several studies have shown a good correlation between the disruption of the photoreceptor inner segment/outer segment (IS/OS) junction and the decrease in visual acuity.[7–10] Ultra–high-resolution OCT, or Fourier-domain (FD) OCT, has an axial resolution of approximately 3 to 5 μm,[9–12] which is significantly better than the axial resolution of approximately 10 μm with the standard OCT. This increased resolution results in better delineation of the retinal architecture and helps in identifying pathologic changes in the microstructure of the retina, especially the photoreceptor layer.[9–11]

A disturbance of IS/OS junction has been reported in cases of postoperative retinal detachment, central serous chorioretinopathy, and retinal dystrophy.[7,8,10,11,13,14] Some studies have found a good correlation between the disturbance of IS/OS junction and the visual acuity.[4,7,10,11]

One problem with conventional OCT is its low transverse resolution. Generally, the transverse resolution of OCT is on the order of 20 μm, which exceeds the cone mosaic spacing of 5 to 10 μm. Two reasons for this limitation are the ocular aberrations and saccadic eye movements. The A-scan technologies adopted in OCT are not suited for obtaining transverse information in both the x- and y-directions in a short acquisition time, and obtaining motion-artifact–free 2-dimesional transverse images of the cone mosaic is not possible.[16]

Adaptive optic (AO) systems seem to be well suited to overcome these problems. An AO system consists of a wavefront sensor to measure ocular aberrations and a de-

ISSN 0161-6420/08/$–see front matter
doi:10.1016/j.ophtha.2008.03.026

formable mirror to compensate for these aberrations. Correcting the ocular aberrations with the AO system can improve the transverse resolution to less than 2 μm, which is necessary to image individual photoreceptors in the living retina.[16–20] Because transverse 2-dimensional images of the retina can be obtained with the AO system, precise detection and measurements of small lesions can be made. Thus, the AO images of patients with cone dystrophy have been reported to have a patchy configuration because of photoreceptor dropout.[21–23] The limitation of the AO system is its low axial resolution. The axial resolution of AO system is approximately 100 μm, even when it is coupled with a scanning laser ophthalmoscope.[19] It is even greater with conventional flood-illumination fundus photography.

Because of the complementary aspects of FD OCT and AO, that is, high axial resolution with FD OCT and high transverse resolution with the AO system, it theoretically would be valuable to combine both instruments to evaluate small focal photoreceptor disruptions. However, the authors have not found a publication that used both systems to compare the images obtained with FD OCT and those obtained with the AO system. The authors have developed a compact, clinically friendly AO fundus camera using a liquid crystal phase modulator. With this instrument, they have been able to show the increased cone spacing in myopic eyes.[24] The purpose of this study was to determine the cause of dark spots in the fovea of 3 patients with metamorphopsia. In all 3 patients, the fundus appeared ophthalmoscopically normal and the photographs obtained by conventional fundus photography also demonstrated normal results. These retinas were examined with their custom-built AO fundus camera, and the images were compared with the OCT images.

Patients and Methods

Patients

Three consecutive patients who reported metamorphopsia but whose photographs of the ocular fundus by standard fundus photography demonstrated normal results were studied. All patients had visited Osaka University Hospital between January and June 2006. The research protocol was approved by the Institutional Review Board of the Osaka University Medical School, and the procedures conformed to the tenets of the Declaration of Helsinki. After the nature and possible consequences of the study were explained, written informed consent was obtained from all patients.

Procedures

All patients underwent a comprehensive ophthalmologic examination, including the measurement of best-corrected visual acuity (BCVA), Amsler chart, fundus photography, and slit-lamp biomicroscopy of the fundus. They also underwent examinations by FD OCT (RTVue-100; Optovue, Inc., Fremont, CA) and a custom-built AO fundus camera.[24] All 3 patients also underwent fluorescein angiography (FA) and indocyanine green angiography (ICGA).

Adaptive Optic Fundus Camera

A detailed description of the custom-built AO fundus camera has been published.[24] The principle of this flood illumination AO fundus camera was similar to that reported by Roorda and Williams.[17] Briefly, the main components of the camera were a nematic liquid crystal phase modulator (X8267–12; Hamamatsu Photonics, Hamamatsu, Japan), a Hartmann-Shack wavefront sensor (28×28 lenslets; specially made by Topcon, Co., Tokyo, Japan), and a scientific charge-coupled device digital camera (C9100–02; Hamamatsu Photonics).

The wavefront sensor measured the ocular wavefront up to the eighth Zernike order, and the phase modulator compensated for the measured wavefront aberrations. The system also is equipped with coaxial, 8-degree–wide viewing optics to identify the location and orientation of the highly magnified retinal images being observed.

Topical tropicamide (0.5%) and phenylephrine (0.5%) were used to dilate the pupil and to paralyze the ciliary muscle. The retina was illuminated with a 2-ms flash (635-nm wavelength) from a xenon arc lamp, and a retinal image was obtained with a 6-mm–diameter exit pupil. The patient was instructed to fixate a designated location on a target. Frame averaging was performed using custom software (Topcon) to improve the quality of the image. Overlapping images were merged using Photoshop (Adobe Systems, Inc., San Jose, CA). To identify the fovea, a montage of the AO images was made and superimposed on the fundus photographs and the fundus projection of OCT images.

Case Reports

Patient 1. A 39-year-old man reported metamorphopsia in his left eye which began 3 months earlier. His BCVA was 20/15 in both eyes. Ophthalmoscopy showed that the ocular fundus appeared normal in both eyes (Fig 1A). Slit-lamp biomicroscopy showed an irregularly shaped dark spot in the fovea centralis of the left eye. Amsler chart examination showed a localized area of metamorphopsia just below the fixation point.

Fourier-domain OCT demonstrated a disturbance of the IS/OS junction and OS layer (between second and third line of FD OCT) of approximately 330 μm on the horizontal scan and 150 μm on the vertical scan. The external limiting membrane layer was intact (Fig 1B,C).

The AO image showed a dark area, that is, an absence of the cone mosaic, at the fovea just above the fixation point. The shape of dark area was geographic, and the size was approximately 350 μm horizontally and 160 μm vertically (Fig 1D–F).

Patient 2. A 39-year-old man reported blurred vision and metamorphopsia in his right eye of 2 years' duration. His BCVA was 20/60 in the right eye and 20/20 in the left eye. He had been diagnosed with keratoconus in his right eye, but his vision did not improve after wearing a hard contact lens.

The ocular fundus appeared normal in fundus photographs (Fig 2A). Slit-lamp biomicroscopy showed an abnormal reflex in the macula and an irregularly shaped dark spot in the fovea centralis of the right eye. Amsler chart examination showed a central scotoma. Fluorescein angiography and ICGA did not show any abnormal findings (Fig 2B).

Fourier-domain OCT demonstrated a defect in the OS layer in the fovea that was located just under the IS/OS layer. The size of the defect was 280 μm on the horizontal scan and 100 μm on the vertical scan. The IS/OS junction was preserved but the intensity was slightly lower. The external limiting membrane and the RPE layers appeared to be normal (Fig 2C,D).

The AO image indicated a disappearance of the cone mosaic at the fovea. The dark area was oval, and the size was 300 μm horizontally and 120 μm vertically (Fig 2E–G).

Patient 3. A 62-year-old man reported metamorphopsia in his left eye of 6 months' duration. His BCVA was 20/200 in the right eye and 20/22 in the left eye. No abnormality was found in the ocular fundus in the conventional fundus photographs (Fig 3A). Slit-lamp biomicroscopy showed an irregularly shaped dark spot in the fovea centralis of the left eye. Amsler chart examination indicated a localized area of metamorphopsia just below the fixation point. The FA and ICGA results were normal (Fig 3B).

Fourier-domain OCT demonstrated an elevation of the external limiting membrane. The photoreceptor OS and IS/OS junction were not detected over an area of 200 μm on the horizontal scan and 150 μm on the vertical scan (Fig 3C,D).

The AO image demonstrated the disappearance of the cone mosaic at the foveal zone. At the fovea centralis, a relatively high reflective area without cone mosaic was observed. The area of the absence of foveal cones was approximately 300 μm horizontally and 200 μm vertically (Fig 3E,F).

Results

All 3 patients had metamorphopsia unilaterally, and the BCVA ranged 20/200 to 20/15 in the affected eye. The Amsler chart examination showed localized metamorphopsia in 2 eyes and a central scotoma in 1 eye. The ocular fundus appeared to be normal in standard fundus photographs, but slit-lamp biomicroscopy revealed an irregularly shaped dark spot in the fovea centralis in the 3 cases. Fluorescein angiography and ICGA did not show any abnormal findings in any cases.

Fourier-domain OCT demonstrated an absence of the OS and IS/OS junction of the photoreceptors in 1 case and an absence or disturbance of the OS but preservation of the IS/OS junction in 2 cases. The AO images indicated the absence of the cone mosaic in the foveal zone in all 3 cases. The horizontal and vertical sizes of the area of the absence of the photoreceptor mosaic in the AO images in the 3 eyes (400×200 μm, 300×120 μm, and 300×200 μm) were comparable with the sizes of the photoreceptor OS disturbances in the OCT images (330×150 μm, 280×100 μm, 200×150 μm, respectively).

Discussion

This study examined the FD OCT and AO images in patients who showed localized disturbances in the photoreceptor layer. To the best of the authors' knowledge, this is the first study that compares the FD OCT and AO images in the same patient. A localized disappearance of the photoreceptor mosaic was observed in the photographs of the fovea obtained by the AO fundus camera in all 3 cases. The horizontal and vertical sizes of the area of the loss of the photoreceptor mosaic in the AO images were comparable with the area of the OS disturbance in the OCT images. In patient 3, the IS/OS junction and OS were also not detected, but in patients 1 and 2, the IS/OS line was preserved, although the intensity was slightly lower than normal. These results suggested that the dark area seen by slit-lamp biomicroscopy corresponded with an absence of the photoreceptor mosaic in the AO images and with the disturbed photoreceptor OS in the OCT images.

The origin of the high reflectance cone mosaic in the AO fundus camera is reported to be from both the IS/OS junction and the OS in the normal retina.[15] However, based on the results from patient 1, a possibility exists that the OS is more involved in the reflectance of photoreceptor mosaic than the IS/OS junction in the AO images. This hypothesis corresponds with the results of a recent report using AO OCT, in which the cone mosaic is observed clearly at the level of Verhoeff's membrane (the third blight line of FD OCT), where the tip of the cone photoreceptor OS is enveloped by microvilli.[25]

In patients with a macular hole, metamorphopsia is a frequently reported symptom. In the early stage of macular hole, morphologic changes are observed not only in the photoreceptor layer, but also in the inner retinal layers because of the tangential traction on the retinal surface. All of the patients reported metamorphopsia, but the lesion was confined to only the photoreceptor layer and was in a very restricted area in the fovea.

Recently, a new clinical entity termed *foveal spot* or *macular microhole* has been proposed.[26,27] In this lesion, the patient has a mildly reduced visual acuity, a central scotoma, and metamorphopsia, and ophthalmoscopy shows a foveal defect with a red appearance and well-defined margins. The size of the lesion is approximately 100 μm and seems to be intraretinal. Conventional OCT3 images (Stratus model 3000; Carl Zeiss Meditec, Humphrey Division, Dublin, CA) show an abnormality of the outer retina, a defect of retinal pigment epithelium, or both.[27] All 3 of the eyes had an apparently normal ocular fundus by conventional fundus photography, but slit-lamp biomicroscopy showed an irregularly shaped dark spot in the fovea centralis. Thus, the 3 eyes may be included in the category of macular microhole or foveal spot. The decrease in the visual acuity or an increase in the area of metamorphopsia should be reflected in the size of the dark area in AO fundus image, and thus may be helpful to evaluate the progression of a disease quantitatively.

The limitation of this study is that the fovea could not be resolved accurately with the AO system. The AO system allows a transverse resolution of 2 μm, but the photoreceptors in the fovea are smaller than the resolution limit.[16–20] Because of this, it is difficult to identify the individual cones in the fovea centralis in the AO images. However, because the dark area is not observed in the central fovea in normal eyes, the dark area at or around the central fovea can be assumed to be the area of photoreceptor loss or disruption.

In conclusion, the AO fundus camera can acquire 2-dimensional images of the retina with a resolution of approximately 2 μm. This resolution allows the detection of highly localized disturbances of the photoreceptor cells that can correlate with the high-resolution images obtained by FD OCT. Combining the AO fundus camera and FD OCT images can be valuable to assess photoreceptor disruptions, especially in eyes with a small focal foveal lesion. The findings in these 3 patients indicate that patients reporting metamorphopsia may have a localized disruption the of photoreceptor cells in the fovea.